

Comparison of Vitamin C and Its Derivative Antioxidant Activity: Evaluated by Using Density Functional Theory

Yuyang Liu, Chuanqun Liu, and Jianjun Li*



Cite This: *ACS Omega* 2020, 5, 25467–25475



Read Online

ACCESS |



Metrics & More

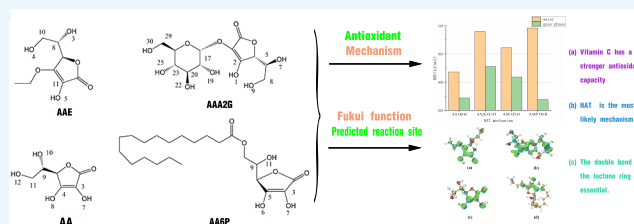


Article Recommendations



Supporting Information

ABSTRACT: Vitamin C (VC) is an essential antioxidant, but its application is limited because of its unstable chemical properties. Hence, a variety of VC derivatives have emerged in practical antioxidant applications. To explore the relationship between the antioxidant properties and the chemical structures of vitamin C and its derivatives, density functional theory (DFT) was used in this work to calculate the reaction enthalpies of the mechanisms related to radical scavenging activity. The structures were optimized at the B3LYP-D3(BJ)/6-31G* level of theory. Single point calculations (SPE) were performed at the PWPB95-D3 (BJ)/def2-QZVPP level. To estimate the solvent effect on antioxidant properties, the SMD (solvation model based on density) method was used. The results showed that in the process of optimizing the chemical structure of vitamin C, the antioxidant capacity of its derivatives decreased slightly in aqueous solvents. In the calculation process, it is also found that in the choice of antioxidant mechanism, these compounds are more inclined to the hydrogen atom transfer (HAT) mechanism, and from the chemical structure point of view, the double bond of the lactone ring is essential for its free radical scavenging activity. In general, it is necessary to continue to optimize the structure of VC to obtain derivatives with better oxidation resistance and more practical value.



INTRODUCTION

Oxidative stress is one of the reasons for promoting the aging of the body and many diseases, and its mechanism is mostly related to the generation of reactive oxygen species (ROS).^{1–5} The generation of ROS is due to the double radical nature of molecular oxygen, which makes it easy to accept electrons, thereby generating free radicals, such as hydroxyl radicals HO•, superoxide radical anions (O₂^{•-}), peroxy radicals (ROO•), hydrogen peroxide (H₂O₂), and alkoxy radicals (RO•), etc.⁶ Substances that eliminate free radicals, also known as the antioxidant capacity of antioxidants, can slow the process of human aging and many diseases to a certain extent.⁷ Therefore, exploring the antioxidant capacity of substances has been a hot topic. Vitamin C (VC), also known as ascorbic acid (AA), is one of the essential trace elements in the human body and considered to be the most effective water-soluble antioxidant.^{8,9} It cannot be synthesized by the body and needs to be supplemented through diet or medicine. Due to their antioxidant capacity, VC and its derivatives have excellent performance in chemical and medical applications. They not only are active ingredients of whitening products but also show therapeutic effects in the treatment of many diseases, including cancer.^{10–19}

There are many ways to compare the antioxidant capacity of antioxidants, but no matter what kind of method is used, the quenching of free radicals is a step that cannot be ignored. AA and its derivatives can certainly quench the free radicals produced by oxidative stress,^{20,21} and the quenching process is

mainly explained by the following three antioxidant mechanisms:^{5,22–24} the hydrogen atom transfer (HAT) mechanism, the single electron transfer proton transfer (SET-PT) mechanism, and the sequential proton loss electron transfer (SPLET) mechanism. The antioxidant efficiency of these mechanisms can be represented by thermochemical parameters, including bond dissociation enthalpy (BDE), adiabatic ionization potential (IP), proton dissociation enthalpy (PDE), proton affinity (PA), and electron transfer enthalpy (ETE).

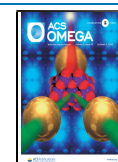
BDE is an important parameter for estimating antioxidant activity in the HAT mechanism.^{5,25–27} IP and PDE represent the two-step process of the SET-PT mechanism. PA and ETE are used to study the SPLET mechanism, as shown in Scheme 1.

Density functional theory (DFT) calculations are often used to analyze the chemical properties of biomolecules (including antioxidant capacity, intermolecular force, and enzyme catalytic ability). Based on the development of DFT computational chemistry in recent years, the current theoretical research results are often used to predict the oxidation resistance of

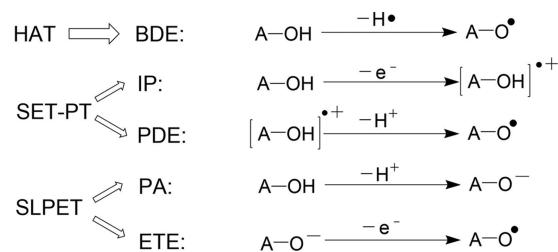
Received: September 4, 2020

Accepted: September 15, 2020

Published: September 25, 2020



Scheme 1. Antioxidant Reaction Mechanism and Corresponding Enthalpy Symbols of VC and Its Derivatives



substances, and the calculations related to the oxidation resistance of VC have also gradually deepened.^{28–31} In practical applications, VC and its derivatives still have a variety of factual problems.^{32–34} For example, the efficient dosage of VC in cancer treatment is very controversial, and related research shows that a low concentration of VC has a certain degree of pro-oxidation, while a high concentration will inhibit the free radical chain reaction. Therefore, a more in-depth exploration of VC and the improvement of its chemical structure to obtain more active and stable derivatives is also an increasingly important direction of study. Compared with its derivatives, such as ascorbyl 2-glucoside (AA2G), 3-*o*-ethyl-L-ascorbic acid (AAE), and ascorbyl 6-palmitate (AA6P), AA has poor molecular stability,^{35–37} and their oxidation strength has not been compared by DFT calculations. Therefore, in this work, DFT calculations were used to evaluate the antioxidant capacity of vitamin C and its derivatives (Figure 1), and the theoretical comparison of antioxidant capacity was carried out to explore the change in the antioxidant capacity of vitamin C in the process of chemical structure optimization and the most probable antioxidant mechanism of these compounds.

RESULTS AND DISCUSSION

To further understand the antioxidant properties of VC and its derivatives, we studied the mechanism of antioxidant activity based on thermodynamic parameters. The reactants and products of the three mechanisms of HAT, SET-PT, and SPLET are the same (Scheme 1), so they should have the same

thermodynamic balance. The competition of the above mechanisms depends on the energy required for each of the key steps. Here, density functional theory is used at the B3LYP/6-31G* level³⁸ in combination with Grimme's DFT-D3,³⁹ and the Becke–Johnson damping function⁴⁰ is used for dispersion correction. The ORCA program⁴¹ used to optimize the conformation of vitamin C and its derivatives, and the accurate single-point energy calculation of the water and gas phases is done at the theoretical level of PWPB95-D3(BJ)⁴²/def2-QZVPP. The most stable structures of VC and its three derivatives in the air (gas phase) and water (aqueous phase) (Figure 2) are used for the further calculation of thermodynamic parameters (BDE, IP, PDE, AP, and ETE).

HAT Mechanism. The principal factor in the ability of antioxidants to scavenge free radicals is their chemical structure. VC and its derivatives (AA2G, AAE, and AA6P) have multiple hydroxyl groups, which is very important for their antioxidant properties. As is known to all, BDE is an important parameter related to the HAT mechanism.²⁶ The lower the BDE value, the lower the stability of the corresponding O–H bond, which indicates that the O–H bond is more accessible to break, that is, the smaller the BDE of the bond, the stronger the oxidation resistance of the substance.

As shown in Figure 3, in the gas phase, the BDE values of various substances are in the order AA6P < AA < AAE < AA2G, and in the aqueous phase, the order is AA < AAE < AA2G < AA6P. The comparison of BDE values between AA and AA6P is consistent with the experimental results of Amorati et al.⁴³ Therefore, in terms of the HAT mechanism in the gas or liquid phase, AA2G is relatively underprivileged in oxidation resistance, while AA has the highest oxidation resistance in the aqueous phase, and AA6P has the highest antioxidant potential in the gas phase. As shown in Table S1, the bond dissociation energy of the O–H bond of each substance under the gas phase condition is lower than the corresponding BDE in the liquid phase condition, apart from O7–H bond in the AA molecule, which in the water phase (308.9 kJ/mol) is lower than its BDE value in the gas phase (323.2 kJ/mol). That is to say, the water solvent can

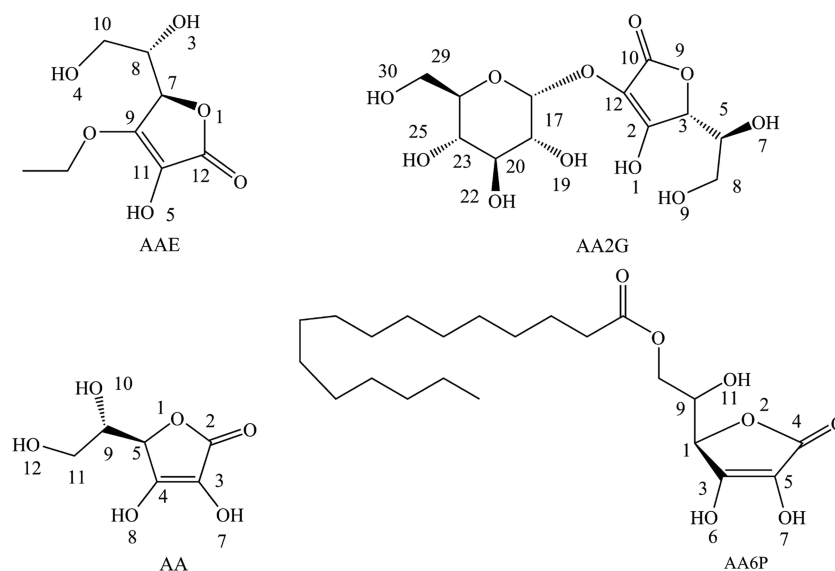


Figure 1. Schematic structures of VC and its derivatives.

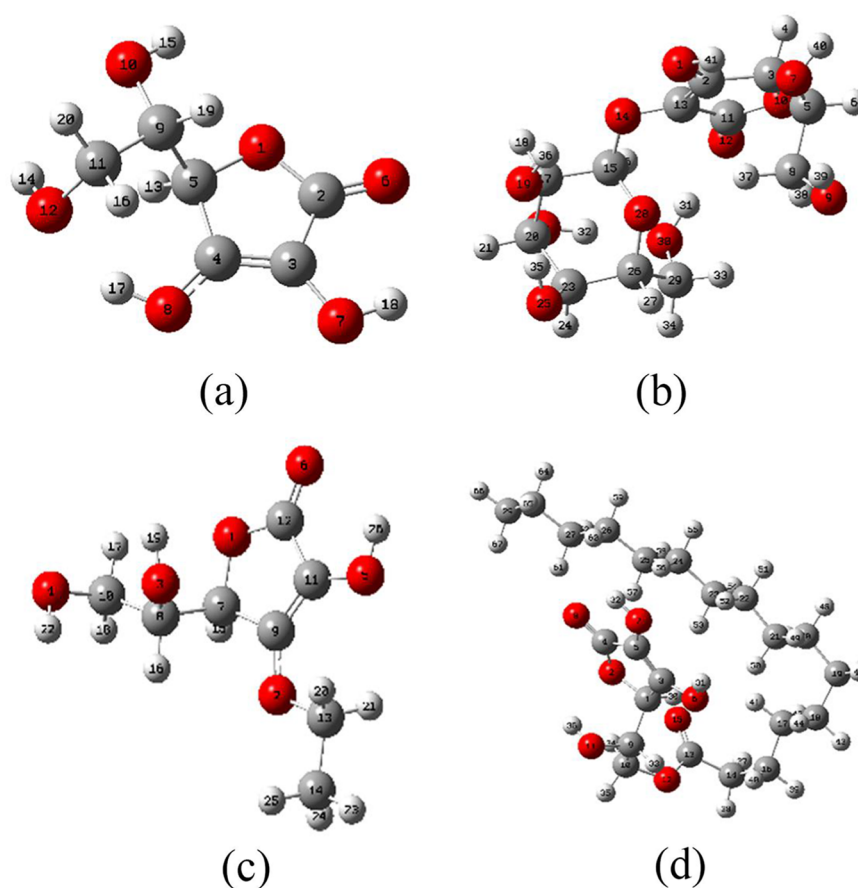


Figure 2. Optimized structure of VC (a), AA2G (b), AAE (c), and AA6P (d) in the gas phase.

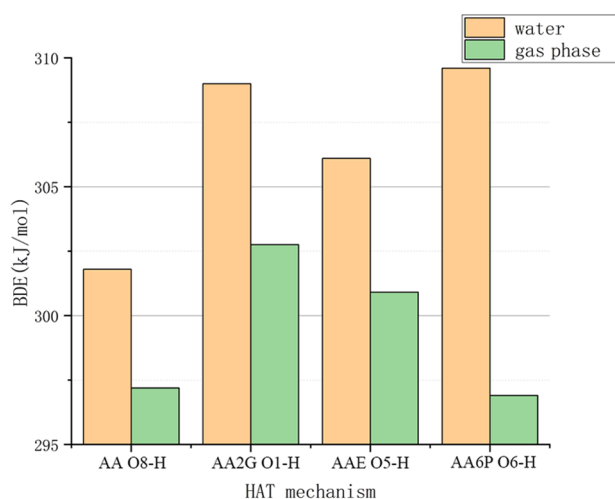


Figure 3. Comparison of bond dissociation enthalpies (BDEs) of VC and its derivatives.

prevent VC and its derivatives from quenching free radicals through the HAT mechanism.

A phenomenon is detected from the calculation results: the hydroxyl groups with the lowest BDE values of VC and its derivatives are all on the lactone ring, and the C atoms connected to these hydroxyl groups have a double bond structure. When the hydroxyl group on the lactone ring loses H atoms to form free radicals, the conjugated double bond provides a resonance environment for unpaired single electrons. Single electrons are delocalized on the lactone

ring, enabling the stable structures of free radicals.⁴⁴ As shown in Figure 4, the spin population distribution of the free radicals formed by the cleavage of O8–H and O7–H bonds in AA molecules, unpaired single electrons, is mainly distributed on the lactone ring, especially on the hydroxyl group, the C atom that is bonded to the hydroxyl group, and the carbonyl group. The use of unrestricted open shells in the calculation will cause the α and β spin orbits to mismatch. The shapes of the two sets of orbits slightly deviate, and two spin states will appear even when the spin multiplicity is 2. As shown in Figure 4, the spin direction represented by blue is relatively weak, so it can be ignored. The singly occupied molecular orbital (SOMO) orbit contributes to all the spin populations.

It is worth noting that AA and AA6P both have two hydroxyl groups on the lactone ring. The BDE value of AA6P's O6–H bond is lower than that of O7–H, regardless of the water phase or gas phase conditions. The BDE values under gas and liquid phase conditions differed by 10.019 and 1.258 kJ/mol, respectively. The BDE value of O8–H in the AA molecule is also lower than that of O7–H in different phases. The difference is 7.11 kJ/mol in the water phase and 26.052 kJ/mol in the gas phase. It shows that under the liquid phase conditions, due to the polarization of water, it will reduce the difference between the BDE values of the two hydroxyl groups on the AA and AA6P lactone rings. The spin population (Figure 4) of AA–O7–H free radicals breaking in water is wider with better delocalization of single electrons; the spin population distribution on O7, O8, and C4 decreases, and the spin layout on O1, C2, C3, and O6 increases, inducing a lower BDE value of O7–H in aqueous simulated media. For the

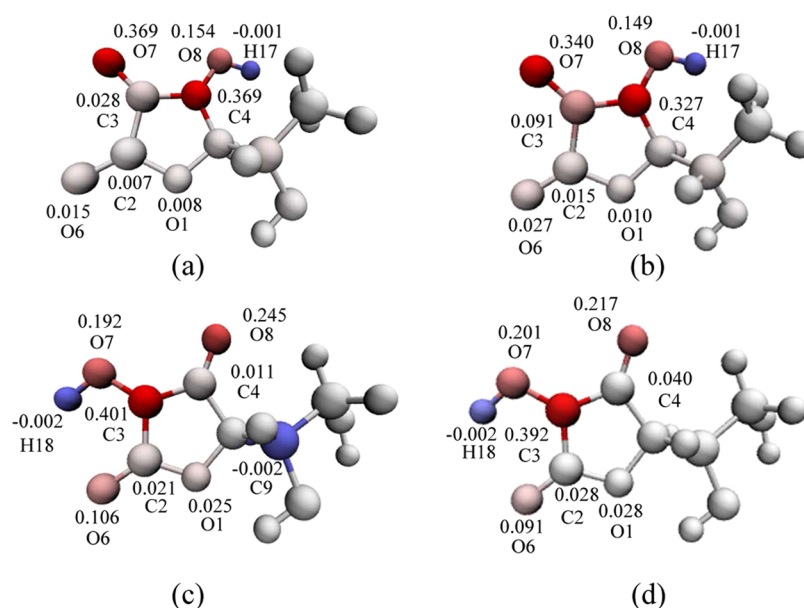


Figure 4. Spin population distribution in the radical species of AA. (a, b) Spin population distribution of the radicals formed by the cleavage of O7–H bond in the gas phase and the water phase, respectively. (c, d) Spin population distribution of the radicals formed by the cleavage of O8–H bond in the gas phase and the water phase, respectively. Red and blue indicate two spins in different directions.

O8–H radical, the spin population does not show a large decrease in the value, but an increase in the small value, and the value becomes smaller for O6 and O8, resulting in a slight increase in BDE in water.

SET-PT Mechanism. IP and PDE values are the enthalpies of the reaction related to the SET-PT mechanism. In the mechanism of SET-PT, antioxidant transfer electrons form free radical cations, which subsequently cause their protonation or deprotonation. IP is the energy of cationic radicals minus the energy of neutral molecules, which can reflect the overall electron-donating ability of molecules. Its influencing factors mainly depend on the degree of conjugation of the system and the electronic effect of the substituent. The lower the IP value, the easier the electron transfer reaction proceeds, and the stronger the antioxidant activity of the substance. Therefore, IP can well represent the antioxidant activity of the substance in the mechanism of SET-PT.

As shown in Figure 5, the sequence of the IP values of various substances in the gas phase is $AAE < AA6P < AA < AA2G$, and in the water phase, it is $AA < AAE < AA2G < AA6P$. As far as the SET-PT mechanism is concerned, AA is more accessible to give electrons in polar solvents and has the strongest resistance to oxidation. Compared with gas, the IP value of VC and its derivatives in water is lowered by about 173–222 kJ/mol (Table S2). It shows that VC and its derivatives are more likely to lose electrons in the water phase.

The calculated PDE values in polar solvents (water phase) (Table S3) are lower than the corresponding IP values (Table S2). Because the energy required for the deprotonation of radical cations ($ROH^{\bullet+}$) in polar solvents is greater than the energy required for the first step of SET-PT, the IP and PDE values of VC and its derivatives can be mutually verified. As shown in Figure 6, the sequence of the calculated PDE values in the gas phase is $AAE < AA6P < AA < AA2G$, and in the water phase, it is $AA < AAE < AA2G < AA6P$.

The antioxidation result of the SET-PT mechanism is obtained by the energy of two steps, that is, the result of the calculation by $IP + PDE$ (shown in Figure 7). As shown in the

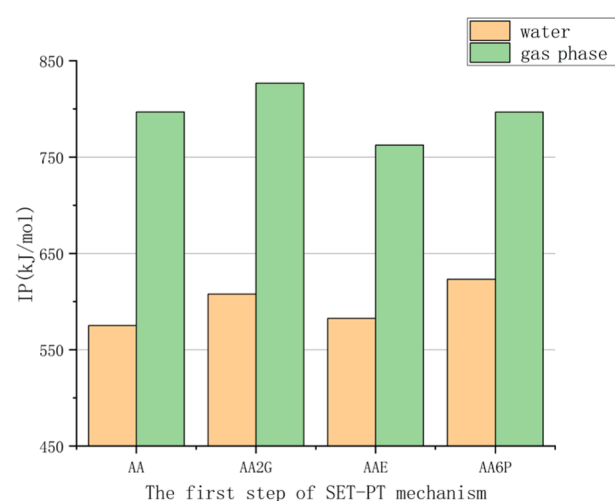


Figure 5. Comparison of the adiabatic ionization potentials (IPs) of VC and its derivatives.

above calculation results, irrespective of water or gas, the calculated IP value of each substance (575.0–826.7 kJ/mol) is higher than the corresponding BDE value (301.8–409.3 kJ/mol). Therefore, it is speculated thermodynamically that the SET-PT mechanism is less likely to occur than the HAT mechanism. Moreover, related research shows that the radical cation of VC is kinetically unstable,²⁹ which is relatively unfavorable for the mechanism of SET-PT. Of course, from theoretical calculations, the antioxidant capacity of VC derivatives is worse than that of VC in the SET-PT mechanism because the sum of the IP and PDE values of VC is the smallest (Figure 8).

SPLET Mechanism. The first step of the SPLET mechanism is the process of antioxidant deprotonation (generation of $A-O^-$), which is often represented by the value of proton affinity (Table S4). The order of the PA values of VC and its derivatives (shown in Figure 8) is $AA2G < AA <$

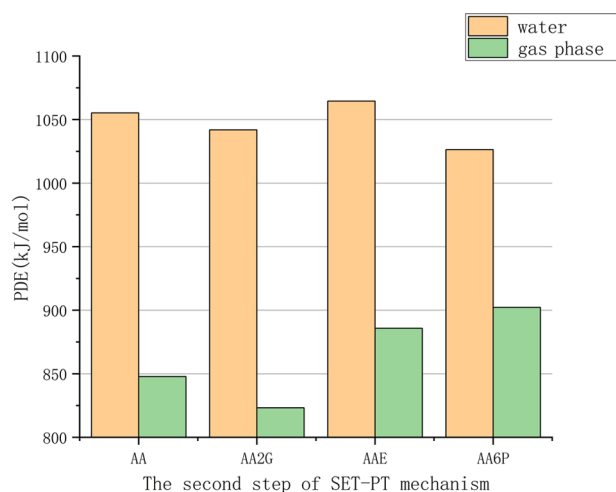


Figure 6. Comparison of the proton dissociation enthalpies (PDEs) of VC and its derivatives.

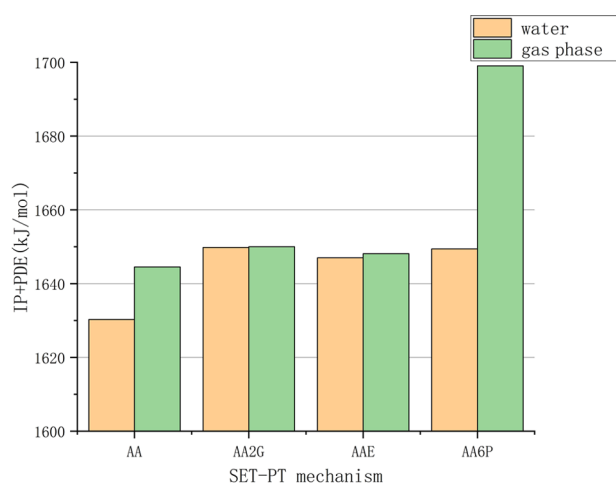


Figure 7. Comparison of the sum of IP and PDE values for VC and its derivatives.

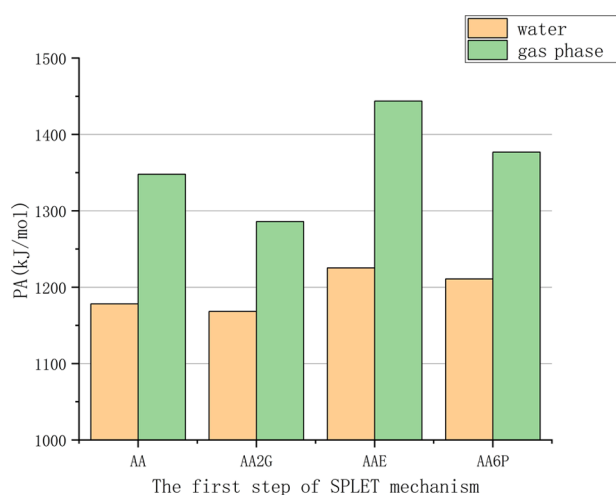


Figure 8. Comparison of the proton affinities (PAs) of VC and its derivatives.

AA6P < AAE, which is the result in both the water phase and the gas phase.

It is worth noting that the proton affinity of the hydroxyl group (AA-O7-H and AA-O8-H) on the lactone ring of VC is higher than that of AA-O12-H and AA-O10-H, which is very different from the three derivatives of AA (AAE, AA2G, and AA6P). By comparing the initial structure of AA-O12-H and AA-O10-H proton loss and the final optimized structure (as shown in Figure 8), it was detected that when the proton transfer of O10-H and O12-H occurs, the conformation of AA changes greatly. When O10-H loses a proton, the proton on O12 is subsequently transferred to O10, and the proton on O8 is transferred to O12. The final stable conformation is actually that O8 loses a proton, and in this conformation, O10-H...O12 and O12-H...O8 form intramolecular hydrogen bonds, resulting in the fact that the conformation formed after the deprotonation of O10-H is more stable than that formed after the direct deprotonation of O8-H. Therefore, the Gibbs free energy of O10-H deprotonation is lower than that of O8-H deprotonation. Similarly, when O12-H loses a proton, it is also found that during the optimization process, the H on O8 is transferred to O12 and O12-H...O8 forms intramolecular hydrogen bonds. Here, by comparing the initial conformation, it can be found that O12-H and O10-H have the lowest energy to overcome the proton loss of O8, which means that the O atom of the double bond on the lactone ring is more chemically reactive. This result is similar to that of the HAT mechanism, suggesting that the double bond of lactone is very important for the antioxidant capacity of VC and its derivatives. Some experimental results also suggest that the antioxidant activity of AA2G comes from the lactone ring of VC rather than from glucose, which is consistent with the above results.⁴⁵

A-O- is generated in the first step of SPLET, and the second step exhibits electron transfer. Electron transfer enthalpy is adopted to study the antioxidant efficiency of this step. The ETE values (shown in Table S5) of VC and its derivatives in the water phase are in the order (Figure 9) AA < AAE < AA6P < AA2G. Relatively speaking, the sequence in the gas phase is AAE < AA2G < AA < AA6P.

Among these substances, AAE has a higher PA, but a relatively lower ETE. Therefore, from a thermodynamic point of view, the deprotonated form of AAE should be the best electron donor. The SPLET mechanism is the sum of the

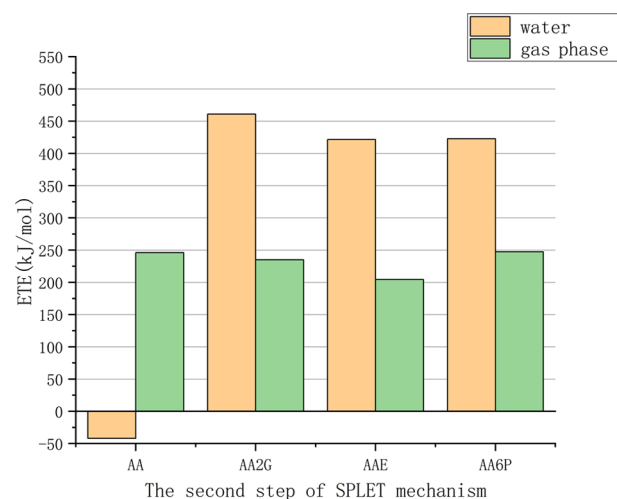


Figure 9. Comparison of the electron transfer enthalpies (ETEs) of VC and its derivatives.

effects of PA and ETE, and owing to the SPLET process affected by environmental acidity and electron-withdrawing groups, the result of the comparison of the oxidation resistance of various substances in this aqueous phase is that VC has the best oxidation resistance. AAE is followed by AA6P, while AA2G is less resistant to oxidation.

As shown in Table S5, the ETE of each substance increases in the gas phase compared to the water solvent, indicating that the energy requirement for anion radicalization in the solvent increases. In addition to the O12 of VC, the consideration is because its position is far away from the lactone ring, and its PA value is much larger than the other spots of VC, but the total PA + ETE quantity (Figure 10) is relatively small, so in

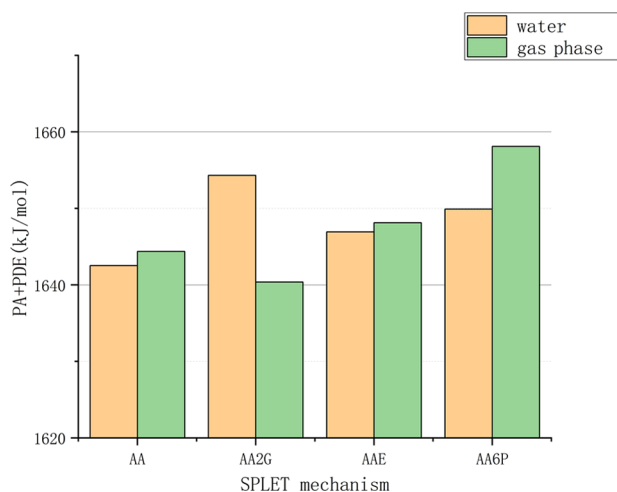


Figure 10. Comparison of the sum of PA and ETE for VC and its derivatives.

general, the solvent will make anionic radicals the demand for chemical energy has increased. Irrespective of gas or water, the ETE value of the reaction of each substance is less than the corresponding IP value, indicating that the ability of neutral molecules to extract electrons is less than that of anions.

From Table S6, it is observed that the total energy requirements of VC and its derivatives related to the HAT mechanism (BDE) are much lower than that of the SPLET mechanism (PA + ETE). Therefore, from the thermodynamic point of view, the antioxidant mechanism of VC and its derivatives is more inclined to hydrogen atom transfer.

Potential Energy Surfaces. To study the antioxidant effect of VC and its derivatives on HO^\bullet radical, we used the Fukui⁴⁶ function to predict the reaction site. As shown in Figure 11, the C=C double bond on the lactone ring and the O functional group on the hydroxyl group are the free radical attack sites. From the above calculation and comparison, it is speculated that the most likely antioxidant mechanism of VC and its derivatives is the HAT mechanism (because the BDE value is relatively small), and the sites that are more likely to react with free radicals are AA-O8, AA2G-O1, AAE-O5, and AA6P-O6, which are the hydroxyl groups with the lowest BDE values of VC and its derivatives. Therefore, to better explore the antioxidant capacity of these substances, we continue to calculate the reaction of these hydroxyl groups with HO^\bullet free radicals in aqueous simulated media.

The potential energy surface (PES) of the reaction of the above substances with the HO^\bullet group in water is displayed in Figure 12. It shows that VC is most likely to react with HO^\bullet groups (-109.237 kJ/mol) to form free radical adducts, indicating that VC has the advantage of free radical scavenging compared to its derivatives. However, from the calculation results of the transition state (TS), VC and its derivatives can

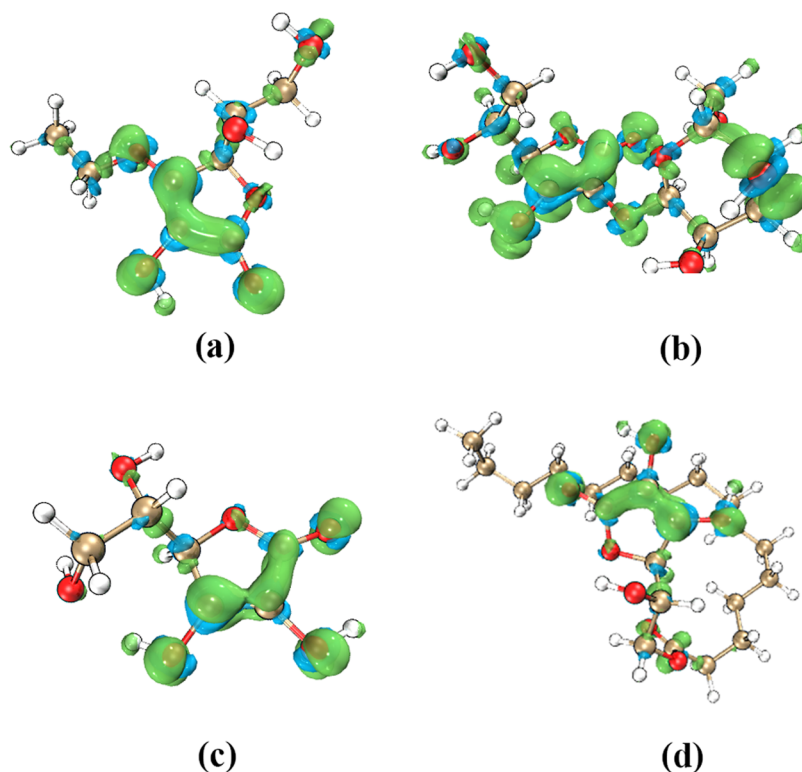


Figure 11. Surface plot of the Fukui function of $f^0(r)$ of VC (a), AA2G (b), AAE (c), and AA6P (d).

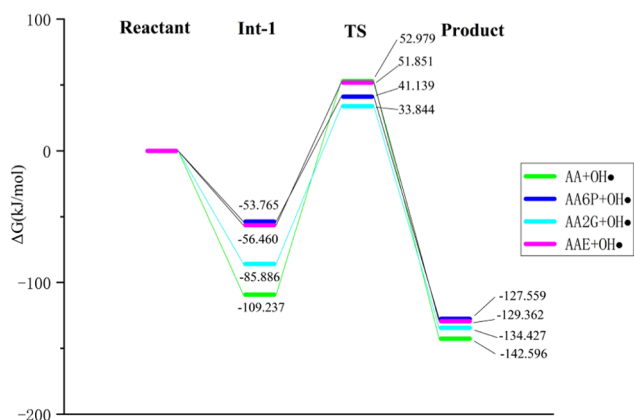


Figure 12. Potential energy surfaces (PES) of the reaction between VC and its derivatives with the HO[•] group in water.

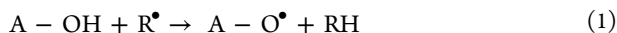
easily eliminate the HO[•] group by the reaction because the energy of this process is not high (33.844–52.979 kJ/mol). AA needs to overcome the highest energy barrier of 162.216 kJ/mol to form H₂O, so the process is kinetically unfavorable. But this barrier is calculated at room temperature and the body temperature is about 37 °C, which may help overcome it.

CALCULATION DETAILS

Low-lying isomers are randomly generated using the Molclus program.⁴⁷ This program is designed to search for clusters and molecular conformations. Batch optimization was carried out under the GFN2-xTB of the xtb program package⁴⁸ combined with the implicit water model. Thus, hundreds of isomers are obtained for each molecule. Multiple most stable conformations are obtained, and then ORCA is used in B3LYP-D3(BJ)/6-31G* to reoptimize important conformations, followed by vibration analysis in the gas phase to verify whether it is a local minimum. The transition state (TS) has only one virtual frequency, and the transition state connecting reactants and products is determined by the intrinsic reaction coordinate (IRC). To obtain more reliable thermal correction of the Gibbs free energy, PWPB95-D3 (BJ)/def2-QZVPP was combined with the SMD model to perform the high-precision single-point energy (SPE) calculation for the most stable isomer obtained from each molecule optimization.

The calculation of the following reaction formula is carried out under the condition of $T = 298.15$ K using uncalibrated zero-point energy (ZPE) as the condition.

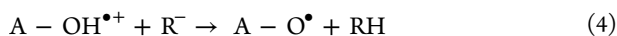
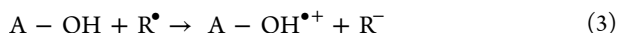
The HAT process is



BDE calculation method is

$$BDE = H(A - O^{\bullet}) + H(H^{\bullet}) - H(A - OH) \quad (2)$$

SET-PT is a two-step reaction, electron transfer followed by protonation of free radical cations, that is

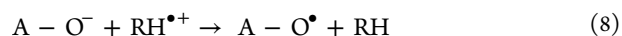


The IP and PDE values represent the above two-step process and are evaluated by the following equations

$$IP = H(A - OH^{\bullet+}) + H(e^{-}) - H(A - OH) \quad (5)$$

$$PDE = H(A - O^{\bullet}) + H(H^{\bullet}) - H(A - OH^{\bullet+}) \quad (6)$$

Similar to SET-PT, the SPLET mechanism is also a two-step process. On the contrary, the SPLET mechanism first converts VC and its derivatives into anions and then transfers electrons to free radicals in the second step



PA and ETE here represent the energy information calculation method of two steps as follows

$$PA = H(A - O^{-}) + H(H^{\bullet}) - H(A - OH) \quad (9)$$

$$ETE = H(A - O^{\bullet}) + H(e^{-}) - H(A - O^{-}) \quad (10)$$

The enthalpies of H(H[•]) and H(e⁻) in the calculation process were 6.197 and 3.145 kJ/mol, respectively.⁴⁹ In the above equations, R[•], A–OH, A–O[•], A–OH^{•+}, and A–O⁻ represent free radicals; VC and its derivatives; and VC and its derivatives in the free radical form, cationic form, and anionic form, respectively.

We used Multiwfn software⁵⁰ for spin populations and Fukui function analysis. The Fukui function $f(r)$ is defined by eq 11.⁴⁶

$$f(r) = \left[\frac{\partial \mu(r)}{\partial v} \right]_N = \left[\frac{\partial \rho(r)}{\partial N} \right]_V \quad (11)$$

$$f^{-}(r) = \left[\frac{\partial \rho(r)}{\partial N} \right]_{v^{-}} \quad (\text{governing electrophilic attack}) \quad (12)$$

$$f^{+}(r) = \left[\frac{\partial \rho(r)}{\partial N} \right]_{v^{+}} \quad (\text{governing nucleophilic attack}) \quad (13)$$

$$f^0(r) = \frac{1}{2} [f^{+}(r) + f^{-}(r)] \quad (\text{free radical attack}) \quad (14)$$

CONCLUSIONS

This theoretical calculation study shows that the oxidation resistance of the derivatives of VC (AA2G, AAE, and AA6P) decreases with the increase of molecular structure stability. By comparing BDE, IP, PDE, PA, and ETE, our results show that no matter what the mechanism (HAT, SET-PT, and SPLET) compares in the aqueous phase, VC has the highest antioxidant performance. The calculated results in the air environment deviate from this, suggesting that the solvent effect influences the antioxidant capacity of VC and its derivatives. We plan to continue to explore the effects of other solvents on the ability of VC and its derivatives to quench free radicals. The HAT mechanism seems to be the most likely mechanism of VC in its free radical scavenging effect. Compared with BDE values, the IP values in the SET-PT mechanism and the PA values in the SPLET mechanism are relatively higher, so it is speculated that the HAT mechanism described by the BDE value is more suitable than the SET-PT and SPLET mechanisms. The results also show that, in the process of quenching radicals, the most likely reaction sites of VC and its derivatives are on the double bond of lactone ring, whether by hydrogen atom transfer, electron transfer, or proton transfer.

Derivatives produced in the process of optimizing the chemical structure of vitamin C are more stable and soluble. This study implies that there is a partial loss of antioxidant

properties of VC derivatives during this process. Therefore, it is particularly important to continue to optimize its chemical structure. In this paper, the calculation and comparison of antioxidant properties of VC and its derivatives wish to provide a new direction for the optimization of the chemical structure of simple vitamins such as VC.

■ ASSOCIATED CONTENT

SI Supporting Information

The Supporting Information is available free of charge at <https://pubs.acs.org/doi/10.1021/acsomega.0c04318>.


Values of thermodynamic parameters related to the antioxidant mechanism of VC and its derivatives calculated in the water and gas phases at the B3LYP/6-31G* level; and optimized geometries of TS in the reaction between VC and its derivatives with OH[•] (PDF)

■ AUTHOR INFORMATION

Corresponding Author

Jianjun Li – Department of Orthopedics, Shengjing Hospital of China Medical University, Shenyang 110004, China;
Phone: +86-18940259895; Email: lij2046@126.com

Authors

Yuyang Liu – Department of Orthopedics, Shengjing Hospital of China Medical University, Shenyang 110004, China;
 orcid.org/0000-0003-3973-0177

Chuanqun Liu – School of Energy and Power Engineering, Northeast Electric Power University, Jilin 132000, China

Complete contact information is available at:

<https://pubs.acs.org/doi/10.1021/acsomega.0c04318>

Notes

The authors declare no competing financial interest.

■ ACKNOWLEDGMENTS

The authors are grateful for financial support from the National Natural Science Foundation of China (81972829), Shengjing Hospital of China Medical University, and Northeast Electric Power University.

■ REFERENCES

- (1) Masaki, H. Role of antioxidants in the skin: anti-aging effects. *J. Dermatol. Sci.* **2010**, *58*, 85–90.
- (2) Di Meo, S.; Reed, T. T.; Venditti, P.; Victor, V. M. Role of ROS and RNS sources in physiological and pathological conditions. *Oxid. Med. Cell. Longevity* **2016**, *2016*, 1245049.
- (3) Wadhwa, R.; Gupta, R.; Maurya, P. K. Oxidative stress and accelerated aging in neurodegenerative and neuropsychiatric disorder. *Curr. Pharm. Des.* **2018**, *24*, 4711–4725.
- (4) Liguori, I.; Russo, G.; Curcio, F.; Bulli, G.; Aran, L.; Della-Morte, D.; Gargiulo, G.; Testa, G.; Cacciatore, F.; Bonaduce, D.; et al. Oxidative stress, aging, and diseases. *Clin. Interventions Aging* **2018**, *13*, 757.
- (5) Esfandi, R.; Walters, M. E.; Tsopmo, A. Antioxidant properties and potential mechanisms of hydrolyzed proteins and peptides from cereals. *Heliyon* **2019**, *5*, No. e01538.
- (6) Brand, M. D. The sites and topology of mitochondrial superoxide production. *Exp. Gerontol.* **2010**, *45*, 466–472.
- (7) Pan, Y.; Lin, Z. *Anti-aging Effect of Ganoderma (Lingzhi) with Health and Fitness*; Springer, 2019; Vol. 1182, pp 299–309.
- (8) Frei, B.; England, L.; Ames, B. N. Ascorbate is an outstanding antioxidant in human blood plasma. *Proc. Natl. Acad. Sci. U.S.A.* **1989**, *86*, 6377–6381.
- (9) Chen, Q.; Espey, M. G.; Sun, A. Y.; Lee, J.-H.; Krishna, M. C.; Shacter, E.; Choyke, P. L.; Pooput, C.; Kirk, K. L.; Buettner, G. R.; et al. Ascorbate in pharmacologic concentrations selectively generates ascorbate radical and hydrogen peroxide in extracellular fluid in vivo. *Proc. Natl. Acad. Sci. U.S.A.* **2007**, *104*, 8749–8754.
- (10) Elmore, A. R. Final report of the safety assessment of L-Ascorbic Acid, Calcium Ascorbate, Magnesium Ascorbate, Magnesium Ascorbyl Phosphate, Sodium Ascorbate, and Sodium Ascorbyl Phosphate as used in cosmetics. *Int. J. Toxicol.* **2005**, *24*, 51–111.
- (11) Mohamed, R.; Tarannum, S.; Yariswamy, M.; Vivek, H. K.; Siddesha, J. M.; Angaswamy, N.; Vishwanath, B. S. Ascorbic acid 6-palmitate: a potent inhibitor of human and soybean lipoxygenase-dependent lipid peroxidation. *J. Pharm. Pharmacol.* **2014**, *66*, 769–778.
- (12) Amirlak, B.; Mahedia, M.; Shah, N. A clinical evaluation of efficacy and safety of hyaluronan sponge with vitamin C versus placebo for scar reduction. *Plast. Reconstr. Surg. Glob. Open* **2016**, *4* (7), No. e792.
- (13) Hill, A.; Wendt, S.; Benstoem, C.; Neubauer, C.; Meybohm, P.; Langlois, P.; Adhikari, N. K.; Heyland, D. K.; Stoppe, C. Vitamin C to improve organ dysfunction in cardiac surgery patients: review and pragmatic approach. *Nutrients* **2018**, *10*, 974.
- (14) Nauman, G.; Gray, J. C.; Parkinson, R.; Levine, M.; Paller, C. J. Systematic review of intravenous ascorbate in cancer clinical trials. *Antioxidants* **2018**, *7*, 89.
- (15) Taira, N.; Katsuyama, Y.; Yoshioka, M.; Muraoka, O.; Morikawa, T. Structural requirements of alkylglyceryl-L-ascorbic acid derivatives for melanogenesis inhibitory activity. *Int. J. Mol. Sci.* **2018**, *19*, 1144.
- (16) Isola, G.; Polizzi, A.; Muraglie, S.; Leonardi, R.; Lo Giudice, A. Assessment of vitamin C and antioxidant profiles in saliva and serum in patients with periodontitis and ischemic heart disease. *Nutrients* **2019**, *11*, 2956.
- (17) Mešćić Macan, A.; Gazivoda Kraljević, T.; Raić-Malić, S. Therapeutic perspective of vitamin C and its derivatives. *Antioxidants* **2019**, *8*, 247.
- (18) Miao, F.; Su, M.-Y.; Jiang, S.; Luo, L.-F.; Shi, Y.; Lei, T.-C. Intramelanocytic acidification plays a role in the antimelanogenic and antioxidative properties of vitamin C and its derivatives. *Oxid. Med. Cell. Longevity* **2019**, *2019*, 1–14.
- (19) Maekawa, T.; Uchida, T.; Nakata-Horiuchi, Y.; Kobayashi, H.; Kawachi, S.; Kinoshita, M.; Saitoh, D.; Sato, S. Oral ascorbic acid 2-glucoside prevents coordination disorder induced via laser-induced shock waves in rat brain. *PLoS One* **2020**, *15*, No. e0230774.
- (20) Gašperlin, M.; Gosenca, M. Main approaches for delivering antioxidant vitamins through the skin to prevent skin ageing. *Expert Opin. Drug Delivery* **2011**, *8*, 905–919.
- (21) Yim, S.; Lee, J.; Jo, H.; Scholten, J.; Willingham, R.; Nicoll, J.; Baswan, S. M. Chrysanthemum morifolium extract and Ascorbic Acid-2-Glucoside (AA2G) blend inhibits UVA-induced delayed cyclobutane pyrimidine dimer (CPD) production in melanocytes. *Clin. Cosmet. Invest. Dermatol.* **2019**, *12*, 823.
- (22) Pandithavidana, D. R.; Jayawardana, S. B. Comparative Study of Antioxidant Potential of Selected Dietary Vitamins; Computational Insights. *Molecules* **2019**, *24*, 1646.
- (23) Yamabe, S.; Tsuchida, N.; Yamazaki, S.; Sakaki, S. Frontier orbitals and transition states in the oxidation and degradation of L-ascorbic acid: a DFT study. *Org. Biomol. Chem* **2015**, *13*, 4002–4015.
- (24) Kumar, V.; Kishor, S.; Ramaniah, L. M. Understanding the antioxidant behavior of some vitamin molecules: a first-principles density functional approach. *J. Mol. Model.* **2013**, *19*, 3175–3186.
- (25) Vo, Q. V.; Nam, P. C.; Van Bay, M.; Thong, N. M.; Cuong, N. D.; Mechler, A. Density functional theory study of the role of benzylic hydrogen atoms in the antioxidant properties of lignans. *Sci. Rep.* **2018**, *8*, 1–10.

- (26) Szerszunowicz, I.; Klobukowski, J. Characteristics of Potential Protein Nutraceuticals of Plant Origin with Antioxidant Activity. *Molecules* **2020**, *25*, 1621.
- (27) Castro-González, L. M.; Alvarez-Idaboy, J. R.; Galano, A. Computationally Designed Sesamol Derivatives Proposed as Potent Antioxidants. *ACS Omega* **2020**, *5*, 9566–9575.
- (28) Bichara, L. C.; Lanús, H. E.; Nieto, C. G.; Brandán, S. A. Density functional theory calculations of the molecular force field of L-ascorbic acid, vitamin C. *J. Phys. Chem. A* **2010**, *114*, 4997–5004.
- (29) Yadav, R.; Rani, P.; Kumar, M.; Singh, R.; Singh, P.; Singh, N. Experimental IR and Raman spectra and quantum chemical studies of molecular structures, conformers and vibrational characteristics of L-ascorbic acid and its anion and cation. *Spectrochim. Acta, Part A* **2011**, *84*, 6–21.
- (30) Mujika, J. I.; Matxain, J. M. Theoretical study of the pH-dependent antioxidant properties of vitamin C. *J. Mol. Model.* **2013**, *19*, 1945–1952.
- (31) Chen, L.; Liu, C.; Fang, H.; Xie, Q.; Kong, C.; Ji, G.; Xiang, Z. Periodic density functional theory study of the high-pressure behavior of crystalline l-serine-l-ascorbic acid. *J. Mol. Model.* **2016**, *22*, 19.
- (32) Chen, Q.; Espey, M. G.; Sun, A. Y.; Pooput, C.; Kirk, K. L.; Krishna, M. C.; Khosh, D. B.; Drisko, J.; Levine, M. Pharmacologic doses of ascorbate act as a prooxidant and decrease growth of aggressive tumor xenografts in mice. *Proc. Natl. Acad. Sci. U.S.A.* **2008**, *105*, 11105–11109.
- (33) Berger, M. M.; Oudemans-van Straaten, H. M. Vitamin C supplementation in the critically ill patient. *Curr. Opin. Clin. Nutr. Metab. Care* **2015**, *18*, 193–201.
- (34) Taira, N.; Katsuyama, Y.; Yoshioka, M.; Okano, Y.; Masaki, H. 3-O-Glyceryl-2-O-hexyl ascorbate suppresses melanogenesis by interfering with intracellular melanosome transport and suppressing tyrosinase protein synthesis. *J. Cosmet. Dermatol.* **2018**, *17*, 1209–1215.
- (35) Frei, B.; Lawson, S. Vitamin C and cancer revisited. *Proc. Natl. Acad. Sci. U.S.A.* **2008**, *105*, 11037–11038.
- (36) Chen, X.; Liu, R.; Liu, X.; Xu, C.; Wang, X. L-ascorbic Acid-2-Glucoside inhibits *Helicobacter pylori*-induced apoptosis through mitochondrial pathway in Gastric Epithelial cells. *Biomed. Pharmacother.* **2018**, *97*, 75–81.
- (37) Iliopoulos, F.; Sil, B. C.; Moore, D. J.; Lucas, R. A.; Lane, M. E. 3-O-ethyl-l-ascorbic acid: Characterisation and investigation of single solvent systems for delivery to the skin. *Int. J. Pharm. X.* **2019**, *1*, No. 100025.
- (38) Jain, R.; Ahuja, B.; Sharma, B. Density-Functional Thermochemistry. III. The Role of Exact Exchange. *Indian J. Pure Appl. Phys.* **2004**, *42*, 43–48.
- (39) Grimme, S.; Antony, J.; Ehrlich, S.; Krieg, H. A consistent and accurate ab initio parametrization of density functional dispersion correction (DFT-D) for the 94 elements H-Pu. *J. Chem. Phys.* **2010**, *132*, No. 154104.
- (40) Grimme, S.; Ehrlich, S.; Goerigk, L. Effect of the damping function in dispersion corrected density functional theory. *J. Comput. Chem.* **2011**, *32*, 1456–1465.
- (41) Neese, F. The ORCA program system. *Wiley Interdiscip. Rev.: Comput. Mol. Sci.* **2012**, *2*, 73–78.
- (42) Goerigk, L.; Grimme, S. Efficient and Accurate Double-Hybrid-Meta-GGA Density Functionals Evaluation with the Extended GMTKN30 Database for General Main Group Thermochemistry, Kinetics, and Noncovalent Interactions. *J. Chem. Theory Comput.* **2011**, *7*, 291–309.
- (43) Amorati, R.; Pedulli, G. F.; Valgimigli, L. Kinetic and thermodynamic aspects of the chain-breaking antioxidant activity of ascorbic acid derivatives in non-aqueous media. *Org. Biomol. Chem.* **2011**, *9*, 3792–3800.
- (44) Anouar, E. H.; Shah, S. A. A.; Hassan, N. B.; Moussaoui, N. E.; Ahmad, R.; Zulkefeli, M.; Weber, J.-F. F.; et al. Antioxidant activity of hispidin oligomers from medicinal fungi: A DFT study. *Molecules* **2014**, *19*, 3489–3507.
- (45) Takebayashi, J.; Tai, A.; Gohda, E.; Yamamoto, I. Characterization of the radical-scavenging reaction of 2-O-substituted ascorbic acid derivatives, AA-2G, AA-2P, and AA-2S: a kinetic and stoichiometric study. *Biol. Pharm. Bull.* **2006**, *29*, 766–771.
- (46) Parr, R. G.; Gazquez, J. L. Hardness functional. *J. Phys. Chem. A* **1993**, *97*, 3939–3940.
- (47) Lu, T. *Molclus Program*. Version 1.5, 2019.
- (48) Bannwarth, C.; Ehlert, S.; Grimme, S. GFN2-xTBAn accurate and broadly parametrized self-consistent tight-binding quantum chemical method with multipole electrostatics and density-dependent dispersion contributions. *J. Chem. Theory Comput.* **2019**, *15*, 1652–1671.
- (49) Bartmess, J. E. Thermodynamics of the electron and the proton. *J. Phys. Chem. B* **1994**, *98*, 6420–6424.
- (50) Lu, T.; Chen, F. Multiwfn: a multifunctional wavefunction analyzer. *J. Comput. Chem.* **2012**, *33*, 580–592.